

Experiments with neutron beams for the astrophysical s process

This content has been downloaded from IOPscience. Please scroll down to see the full text.

2016 J. Phys.: Conf. Ser. 665 012020

(<http://iopscience.iop.org/1742-6596/665/1/012020>)

View [the table of contents for this issue](#), or go to the [journal homepage](#) for more

Download details:

IP Address: 150.237.202.209

This content was downloaded on 30/03/2016 at 12:39

Please note that [terms and conditions apply](#).

Experiments with neutron beams for the astrophysical s process

C Lederer^{1,2,*}, S Altstadt¹, J Andrzejewski³, L Audouin⁴,
M Barbagallo⁵, V Bécaries⁶, F Bečvář⁷, F Belloni⁸,
E Berthoumieux^{8,9}, J Billowes¹⁰, V Boccone⁹, D Bosnar¹¹,
M Brugger⁹, M Calviani⁹, F Calviño¹², D Cano-Ott⁶, C Carrapiço¹³,
F Cerutti⁹, E Chiaveri^{8,9}, M Chin⁹, N Colonna⁵, G Cortés¹²,
MA Cortés-Giraldo¹⁴, M Diakaki¹⁵, C Domingo-Pardo¹⁶, I Duran¹⁷,
R Dressler¹⁸, N Dzysiuk¹⁹, C Eleftheriadis²⁰, A Ferrari⁹, K Fraval⁸,
S Ganesan²¹, AR García⁶, G Giubrone¹⁶, MB Gómez-Hornillos¹²,
IF Gonçalves¹³, E González-Romero⁶, E Griesmayer²², C Guerrero⁹,
F Gunsing⁸, P Gurusamy²¹, A Hernández-Prieto^{9,12}, DG Jenkins²³,
E Jericha²², Y Kadi⁹, F Käppeler²⁴, D Karadimos¹⁵, N Kivel¹⁸,
P Koehler²⁵, M Kokkoris¹⁵, G Korschinek²⁶, M Krtićka⁷, J Kroll⁷,
C Lampoudis⁸, C Langer¹, E Leal-Cidoncha¹⁷, H Leeb²², LS Leong⁴,
R Losito⁹, A Mallick²¹, A Manousos²⁰, J Marganec³, T Martínez⁶,
C Massimi²⁷, PF Mastinu¹⁹, M Mastromarco⁵, M Meaze⁵,
E Mendoza⁶, A Mengoni²⁸, PM Milazzo²⁹, F Mingrone²⁷, M Mirea³⁰,
W Mondalaers³¹, C Paradela¹⁷, A Pavlik², J Perkowski³,
M Pignatari³², A Plompen³¹, J Praena¹⁴, JM Quesada¹⁴,
T Rauscher³², R Reifarth¹, A Riego¹², MS Robles¹⁷, F Roman^{9,30},
C Rubbia^{9,33}, M Sabaté-Gilarte¹⁴, R Sarmiento¹³, A Saxena²¹,
P Schillebeeckx³¹, S Schmidt¹, D Schumann¹⁸, G Tagliente⁵,
JL Tain¹⁶, D Tarrío¹⁷, L Tassan-Got⁴, A Tsinganis⁹, S Valenta⁷,
G Vannini²⁷, V Variale⁵, P Vaz¹³, A Ventura²⁸, R Versaci⁹,
MJ Vermeulen²³, V Vlachoudis⁹, R Vlastou¹⁵, A Wallner², T Ware¹⁰,
M Weigand¹, C Weiß²², T Wright¹⁰, P Žugec¹¹

¹Johann-Wolfgang-Goethe Universität, Frankfurt, Germany

²University of Vienna, Faculty of Physics, Austria

³Uniwersytet Łódzki, Lodz, Poland

⁴Centre National de la Recherche Scientifique/IN2P3 - IPN, Orsay, France

⁵Istituto Nazionale di Fisica Nucleare, Bari, Italy

⁶Centro de Investigaciones Energeticas Medioambientales y Tecnológicas (CIEMAT), Madrid, Spain

⁷Charles University, Prague, Czech Republic

⁸Commissariat à l'Énergie Atomique (CEA) Saclay - Irfu, Gif-sur-Yvette, France

⁹European Organization for Nuclear Research (CERN), Geneva, Switzerland

¹⁰University of Manchester, Oxford Road, Manchester, UK

¹¹Department of Physics, Faculty of Science, University of Zagreb, Croatia

¹²Universitat Politècnica de Catalunya, Barcelona, Spain

¹³Instituto Tecnológico e Nuclear, Instituto Superior Técnico, Universidade Técnica de Lisboa, Lisboa, Portugal

¹⁴Universidad de Sevilla, Spain



¹⁵National Technical University of Athens (NTUA), Greece

¹⁶Instituto de Física Corpuscular, CSIC-Universidad de Valencia, Spain

¹⁷Universidade de Santiago de Compostela, Spain

¹⁸Paul Scherrer Institut, Villigen PSI, Switzerland

¹⁹Istituto Nazionale di Fisica Nucleare, Laboratori Nazionali di Legnaro, Italy

²⁰Aristotle University of Thessaloniki, Thessaloniki, Greece

²¹Bhabha Atomic Research Centre (BARC), Mumbai, India

²²Atominstitut, Technische Universität Wien, Austria

²³University of York, Heslington, York, UK

²⁴Karlsruhe Institute of Technology, Campus Nord, Institut für Kernphysik, Karlsruhe, Germany

²⁵Department of Physics, University of Oslo, N-0316 Oslo, Norway

²⁶Physik Department E12 and Excellence Cluster Universe, Technische Universität München, Munich, Germany

²⁷Dipartimento di Fisica, Università di Bologna, and Sezione INFN di Bologna, Italy

²⁸Agenzia nazionale per le nuove tecnologie, l'energia e lo sviluppo economico sostenibile (ENEA), Bologna, Italy

²⁹Istituto Nazionale di Fisica Nucleare, Trieste, Italy

³⁰Horia Hulubei National Institute of Physics and Nuclear Engineering - IFIN HH, Bucharest - Magurele, Romania

³¹European Commission JRC, Institute for Reference Materials and Measurements, Retieseweg 111, B-2440 Geel, Belgium

³²Department of Physics and Astronomy - University of Basel, Basel, Switzerland

³³Laboratori Nazionali del Gran Sasso dell'INFN, Assergi (AQ), Italy

*Present Address: School of Physics and Astronomy, University of Edinburgh, UK.

Abstract. Neutron capture cross sections are the key nuclear physics input to study the slow neutron capture process, which is responsible for forming about half of the elemental abundances above Fe. Stellar neutron capture cross section can be measured by the time-of-flight technique, or by activation. Both techniques will be discussed and recent experiments in the Fe/Ni mass region will be presented.

1. Introduction

Neutron capture reactions are the main mechanisms for synthesizing elements heavier than Fe in stars. Two different processes contribute about equally to the overall elemental abundance pattern, the slow neutron capture process (*s* process) and the rapid neutron capture process (*r* process). The *r* process is associated to explosive scenarios with high neutron densities and nuclear reactions involve nuclei far from the stability valley. In the *s* process, heavy elements are produced by subsequent neutron captures on seed nuclei (mainly Fe). Neutron capture timescales are of the order of years, therefore, if an unstable element is produced, β -decays towards the stability valley are faster than subsequent neutron captures. An exception are long lived radionuclides, where β -decay and neutron capture may compete. Such nuclei are called branching points and their study can provide important information such as temperatures and neutron densities in *s* process environments. The *s* process can be further divided in two different components, the main component taking place in thermally pulsing Asymptotic Giant Branch stars, where mainly elements between Zr and Bi are formed, and the weak *s* process which takes place in massive stars ($M > 8M_{\odot}$), where mainly elements between Fe and Zr are produced [1]. The nucleosynthesis path for the *s* process from Fe to Se is illustrated in Figure 1.

The main nuclear physics quantities that are required to study the *s* process are neutron capture cross sections and β -decay half lives. The effective stellar neutron capture cross section, called Maxwellian Averaged Cross Section (MACS), is the energy dependent cross section

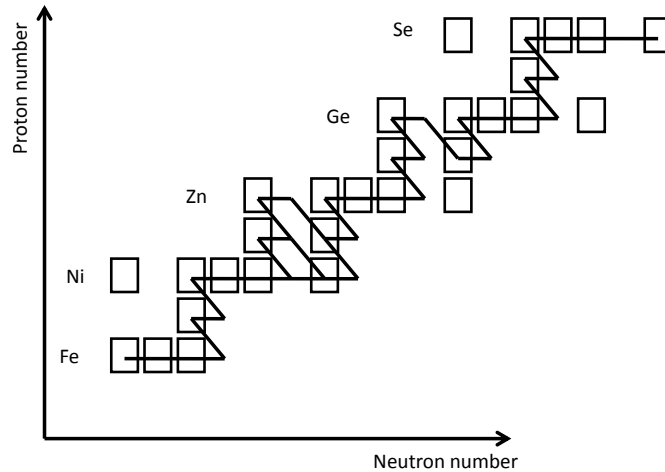


Figure 1. The *s* process nucleosynthesis path starting from Fe, indicated by the black solid line.

averaged over the stellar neutron spectrum and defined as:

$$\langle \sigma \rangle = \frac{2}{\sqrt{\pi}} \frac{1}{(k_B T)^2} \int_0^\infty \sigma(E) E \exp\left(-\frac{E}{k_B T}\right) dE \quad (1)$$

Maxwellian Averaged Cross Sections need to be known over a wide range of kT values (8-100 keV) since *s* process environments exhibit temperatures from 0.1-1 Gigakelvin.

This paper will present neutron capture measurements at the neutron time-of-flight facility n_TOF/CERN in the Fe/Ni mass region.

2. Measuring Neutron Capture Cross sections

There are two complementary techniques to measure stellar neutron cross sections, the time-of-flight technique, and the activation technique.

The time-of-flight technique allows measurement of the energy dependence of the cross section, since the neutron energy is determined via the time-of-flight of the neutron for each capture event. A pulsed neutron beam is produced by reactions of a charged particle beam with a neutron production target. This can be achieved, for example, by spallation reactions (e.g. n_TOF/CERN [2] and LANSCE/Los Alamos [3]), or by photon-induced reactions by bremsstrahlung produced by an electron beam hitting a high Z target (e.g. GELINA/Geel [4]), or by (p, n) reactions using low-energy accelerators (e.g. the Karlsruhe Van de Graaff [1]). Capture reactions are measured by detecting the prompt γ radiation emitted after each capture event. Background effects can be minimized by using isotopically enriched samples, and structure materials with low neutron cross sections. The time-of-flight technique allows measurements of neutron cross sections over a wide energy range, enabling calculation of Maxwellian Averaged Cross Sections for several values of kT from a single experiment.

The activation technique comprises of irradiating a sample with neutrons, and afterwards counting the reaction product. This can be done by decay counting or by direct atom counting

techniques, e.g. Accelerator Mass Spectrometry [5]. The latter is especially suited if the reaction product is long lived and/or the decay is not easily measurable by its radiation. To measure stellar cross sections via activation, a neutron spectrum resembling the stellar distribution is needed. A quasi-stellar spectrum around $kT = 25$ keV can be generated using the ${}^7\text{Li}(p, n)$ reaction with a proton beam of about 2 MeV energy [6, 7, 8]. This possibility was developed by Beer and Käppeler [9] at the Forschungszentrum Karlsruhe and extensively used for measuring stellar (n, γ) cross sections over the entire periodic table (e.g. [6, 10]). Quasi-stellar spectra have been obtained for $kT = 5$ keV [11] using the ${}^{18}\text{O}(p, n)$ reaction and for $kT = 52$ keV [12] using the ${}^3\text{H}(p, n)$ reaction, but both reactions yield significantly reduced intensities. To convert the measured spectrum averaged cross section to a MACS, some assumptions on the energy dependence of the cross section have to be made, but the respective conversion factors are usually close to 1. Besides the limitation that the activation technique can only be applied to reactions producing radioactive nuclei, there are also several advantages compared to the time-of-flight technique. Sample material can be used in natural composition since the reaction is detected either via characteristic γ -ray emission or by directly counting the reaction product. Additionally, small amounts of sample material are sufficient (of the order of mg vs. hundreds of mg to g for the time-of-flight method), since the neutron beam is continuous and the sample can be put close to the neutron source.

3. (n, γ) Measurements at the n_TOF Facility and Astrophysical Implications

In recent years, several neutron capture measurements of interest for the s process have been performed at the neutron-time-of-flight facility n_TOF, CERN. This section will concentrate on measurements in the Fe/Ni mass region. As mentioned in the introduction, masses from Fe to Zr are produced by the weak s process component. It was found that especially in this mass region, neutron capture cross sections of all involved isotopes have to be known with high accuracy because a single cross section can significantly influence the abundances of a number of heavier isotopes [13]. This need has further been underlined by a discrepancy that was found between elemental abundances in ultra-metal-poor stars and calculated abundances in the Sr-Y mass region [14, 15], which led to the suggestion of an additional nucleosynthesis process [16]. Since neutron capture cross sections are a crucial input for these calculated abundances, cross sections should be known with high accuracy for a better study of this discrepancy.

A campaign was started at n_TOF to measure cross sections of all stable isotopes of Fe and Ni. Measurements of (n, γ) reactions on ${}^{54,56,57}\text{Fe}$ [17] and ${}^{58,62}\text{Ni}$ [18, 19] have been completed.

At n_TOF, an intense neutron beam is produced by spallation reactions of a 20 GeV proton bunch of 7 ns width from the CERN-PS with a massive lead target. Around the target is a water layer for cooling and for moderating the initially very energetic neutrons. The resulting neutron spectrum at n_TOF ranges from thermal neutron energies (0.025 eV) to few GeV. The experimental area is located at a distance of 185 m from the neutron target, which ensures a high energy resolution of 3×10^{-4} at 1 eV to 5×10^{-3} at 1 MeV neutron energy [2]. Prompt capture γ rays were detected using a pair of scintillation detectors, filled with deuterated benzene (C_6D_6), which were optimized to a very low sensitivity towards reactions with neutrons [20].

For the ${}^{62}\text{Ni}(n, \gamma)$ reaction, we obtain a MACS at $kT = 25$ keV which is in good agreement with a time-of-flight measurement by Alpizar-Vicente et al. [21] and activation measurements of Nassar et al. [13] and Dillmann et al. [22]. For $kT > 40$ keV, however, our stellar cross sections are systematically smaller than the results of Alpizar-Vicente et al. [21]. The final MACSs has total uncertainties of about 5% at $kT = 30$ keV and 10% at $kT = 100$ keV.

Additionally to the stable Ni isotopes, the neutron capture cross section of the long lived radionuclide ${}^{63}\text{Ni}$, with a half life of 101.2 ± 1.5 years [23] has been measured for the first time [24]. The neutron capture yield measured at n_TOF compared to backgrounds due to presence of ${}^{62}\text{Ni}$ in the sample and due to reactions of neutrons with the empty sample holder

is shown in Figure 2.

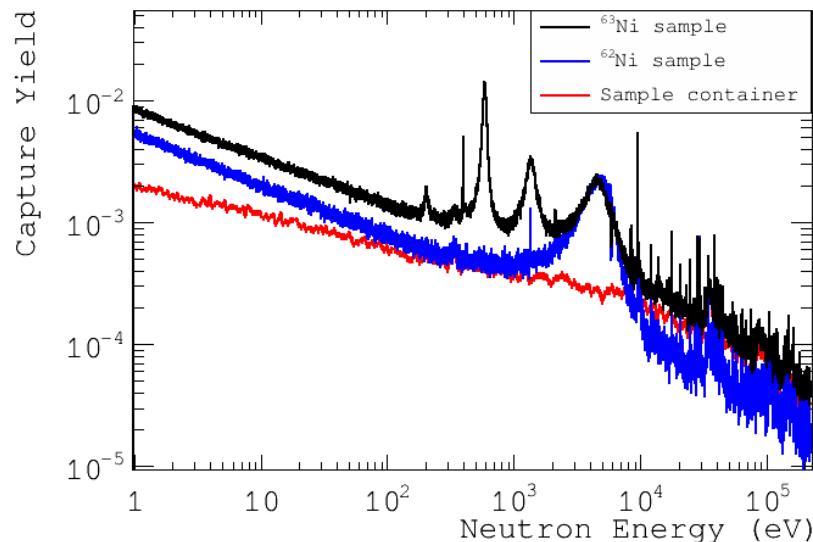


Figure 2. Capture yield of the $^{63}\text{Ni}(n, \gamma)$ reaction measured at n_TOF. The yield is compared to backgrounds coming from reactions on ^{62}Ni , which was present in the sample, and reactions of neutrons with the sample container [24].

^{63}Ni is a branching point in the s process. The weak s process takes place in two different burning stages in massive stars. First, neutrons are produced at the end of helium core burning via the $^{22}\text{Ne}(\alpha, n)$ reaction. The neutron densities around 10^6 cm^{-3} are not sufficient for neutron capture to compete with the decay of ^{63}Ni , which means that the reaction flow is carried only by the decay channel. In the later carbon shell burning phase, the $^{22}\text{Ne}(\alpha, n)$ neutron source is reactivated, leading to several magnitudes larger neutron densities. In this scenario, ^{63}Ni acts like a stable isotope and is mainly depleted via subsequent neutron capture towards ^{64}Ni , bypassing completely the production of ^{63}Cu , which is only produced by β -decay of the ^{63}Ni that is left after the neutron irradiation [25]. We determined stellar cross sections, which were about a factor of 2 higher than previous theoretical estimates listed in the KADoNiS compilation [26]. With the new cross section, we calculated s process abundances of a $25 M_{\odot}$ star and obtained an increase of 20% in the ^{64}Ni abundance and a 15 and 30% decrease of the ^{63}Cu and ^{64}Zn abundances, respectively [24].

4. Outlook

Maxwellian Averaged Cross Sections are an important quantity to study the s process. Most challenging are (n, γ) measurements on radioactive species, since usually only small amounts of sample material are available, as well as measurements of very small (n, γ) cross sections (typically cross sections of light nuclei which may act as neutron poison in the s process). Some of those reactions require higher neutron fluxes than presently available. Several new facilities and upgrades are currently under construction or have been recently completed which are designed to obtain neutron fluxes 10-1000 times higher than existing facilities, e.g. the FRANZ [27] facility at the University of Frankfurt (Germany), SARAF [28] at the Soreq research centre (Israel), and a second experimental area at a shorter flight path at n_TOF [29]. These new facilities

will enable a number of new cross section measurements, e.g. $^{85}\text{Kr}(n, \gamma)$ or $^{204}\text{Tl}(n, \gamma)$, and will provide crucial information for understanding the formation of the heavy elements.

References

- [1] Reifarh R, Lederer C, Käppeler F, *J. Phys. G: Nucl. Part. Phys.* **41**, 053101 (2014).
- [2] Guerrero C, and the n_TOF collaboration, *Eur. Phys. J. A* **49**, 27 (2013), www.cern.ch/ntof
- [3] <http://lansce.lanl.gov/>
- [4] http://irmm.jrc.ec.europa.eu/about_IRMM/laboratories/Pages/gelina_neutron_time_of_flight_facility.aspx
- [5] Wallner A, *Nucl. Instrum. Meth. B* **268**, 1277 (2010).
- [6] Ratynski W and Käppeler F, *Phys. Rev. C* **37**, 595 (1988).
- [7] Lederer C, and the n_TOF Collaboration, *Phys. Rev. C* **85**, 055809 (2012).
- [8] Feinberg G, et al., *Phys. Rev. C* **85**, 055810 (2012).
- [9] Beer H and Käppeler F, *Phys. Rev. C* **21**, 534 (1980).
- [10] Bao Z Y, et al., *At. Data Nucl. Data Tab.* **76**, 70 (2000).
- [11] Heil M, et al., *Phys. Rev. C* **71**, 025803 (2005).
- [12] Käppeler F, Naqvi A, Al-Ouali M, *Phys. Rev. C* **35**, 936 (1987).
- [13] Nassar H, et al., *Phys. Rev. Lett.* **94**, 092504 (2005).
- [14] Sneden C, et al., *Astroph. J.* **467**, 819 (1996).
- [15] Sneden C, et al., *Astroph. J. Lett.* **533**, L139 (2000).
- [16] Travaglio C, et al., *Astroph. J.* **601**, 864 (2004).
- [17] Giubrone G, and the n_TOF Collaboration, in preparation (2014).
- [18] Žugec P, and the n_TOF Collaboration, *Phys. Rev. C* **89**, 014605 (2014).
- [19] Lederer C, and the n_TOF Collaboration, *Phys. Rev. C* **89**, 025810 (2014).
- [20] Plag R, et al., *Nucl. Instrum. Meth. A* **496**, 425 (2003).
- [21] Alpizar-Vicente A M, et al., *Phys. Rev. C* **77**, 015806 (2008).
- [22] Dillmann I, et al., *Nucl. Instrum. Meth. B* **268**, 1283 (2010).
- [23] Colle R, et al., *Appl. Radiat. Isotopes* **66**, 60 (2008).
- [24] Lederer C, and the n_TOF Collaboration, *Phys. Rev. Lett.* **110**, 022501 (2013).
- [25] Pignatari M, et al., *Astroph. J.* **710**, 1557-1577 (2010).
- [26] Dillmann I, et al., *AIP Conf. Proc.* **819**, 123 (2005); online at <http://www.kadonis.org>
- [27] Reifarh R, et al., *Publ. Astr. Soc. Aus.* **26**, 255 (2009).
- [28] Feinberg G, et al., *Nuc. Phys. A* **827**, 590 (2009).
- [29] Chiaveri E, and the n_TOF Collaboration, "Proposal for n_TOF Experimental Area 2 (EAR-2)", CERN-INTC-2012-029 / INTC-O-015 (2012).